

2 **Formulation and characterization of wheat bran oil-in-water**  
3 **nanoemulsions**

4

5 Sara Rebolleda, María Teresa Sanz, José Manuel Benito, Sagrario Beltrán\*, Isabel Escudero  
6 and María Luisa González San-José

7 Department of Biotechnology and Food Science. University of Burgos. Plaza Misael  
8 Bañuelos s/n. 09001 Burgos. Spain.

9 **Abstract**

10 Wheat bran oil (WBO) has been reported to have an important content of bioactive  
11 compounds such as tocopherols, alkylresorcinols, steryl ferulates and other phenolic  
12 compounds; however, its poor solubility in water systems restricts its applications in the food  
13 industry. This study is focused on the formulation of oil-in-water (O/W) nanoemulsions of  
14 WBO in order to improve the bioaccessibility of its active compounds. The influence of oil  
15 concentration, surfactant type and concentration, and emulsification method, on the droplet  
16 size and stability of the nanoemulsions was investigated. Response surface methodology was  
17 used to optimize the conditions for preparing stable nanoemulsions with the minimum droplet  
18 size. The optimal nanoemulsion was obtained when 1% of WBO and 7.3% of a surfactant

---

\* Author to whom correspondence should be addressed. Tel.: +34 947 258810. Fax: + 34 947  
258831. E-mail: [beltran@ubu.es](mailto:beltran@ubu.es)

19 mixture of Span 80 (37.4%) and Tween 80 (62.6%) were emulsified in water by high intensity  
20 ultrasonication for 50 s after pre-emulsification with a high speed blender during 5 min. The  
21 optimal nanoemulsion showed good stability along time and antioxidant and tyrosinase  
22 inhibitory activities, which make it suitable for use in food applications.

## 23 **Keywords**

24 Nanoemulsion. Wheat bran oil. Ultrasonication. Response surface methodology. Antioxidant  
25 capacity. Tyrosinase inhibition.

## 26 **Chemical compounds studied in this article**

27 5-(n-nonadecyl)resorcinol (PubChem CID: 161858);  $\alpha$ -Linolenic Acid (PubChem CID:  
28 5280934);  $\alpha$ -Tocopherol (PubChem CID: 14985);  $\gamma$ -Tocopherol (PubChem CID: 92729);  
29 Tween 80 (polyoxyethylene (20) sorbitan monooleate) (PubChem CID: 5281955); Span 80  
30 (sorbitan monooleate) (PubChem CID: 9920342); Tween 20 (polyoxyethylene (20) sorbitan  
31 monolaurate) (PubChem CID: 443314)

## 32 **1. Introduction**

33 There has been growing interest in the utilization of natural antioxidants in the food, beverage  
34 and pharmaceutical industries due to the increasing consumer's demand for substituting  
35 synthetic compounds by natural substances. Several vegetal by-products have been proved to  
36 be a good source of functional ingredients (Herrero, Cifuentes, & Ibañez, 2006). One of these  
37 by-products is wheat bran, which has been successfully extracted using supercritical fluid  
38 extraction (SFE) giving rise to extracts that have shown an important content on tocopherols,  
39 alkylresorcinols and other phenolic compounds, which provide them with a good antioxidant

40 activity and tyrosinase inhibitory activities (Rebolleda, Beltrán, Sanz, González-Sanjosed, &  
41 Solaesa, 2013; Rebolleda, Beltrán, Sanz, & González-Sanjosed, 2013, 2014).

42 The enzyme tyrosinase is involved both in the browning of food products and in melanosis in  
43 animals. Tyrosinase oxidizes *o*-diphenols to highly reactive *o*-quinones, which can (i)  
44 spontaneously polymerize to form compounds of high molecular weight or brown pigments,  
45 or (ii) undergo nucleophilic attack by amino acids, proteins, polyphenols, or water to form  
46 Michael type addition products, which increase the brown color (Wu, Chang, Chen, Fan, &  
47 Ho, 2009). Therefore, the food industry demands tyrosinase inhibitors to prevent the  
48 alteration of organoleptic and visual quality of food products (Chen, Song, Qiu, Liu, Huang,  
49 & Guo, 2005; Roldán, Sánchez-Moreno, de Ancos, & Cano, 2008; Wu, Chang, Chen, Fan, &  
50 Ho, 2009). Preliminary results obtained in our laboratory showed that wheat bran oil (WBO)  
51 might have an inhibitory effect on mushroom tyrosinase (Rebolleda, Beltrán, Sanz, González-  
52 Sanjosed, & Solaesa, 2013).

53 Due to its lipophilic character, WBO must be formulated before it can be used for aqueous-  
54 based matrix applications. The high stability and low turbidity of nanoemulsions (10-200 nm)  
55 make them suitable to incorporate lipophilic active ingredients in aqueous-based food and  
56 beverages (McClements, 2011; Yang, Marshall-Breton, Leser, Sher, & McClements, 2012).  
57 Furthermore, nanoemulsions have been described as drug delivery systems and as adequate  
58 media to overcome instability and to enhance the bioavailability of nutraceuticals (Huang, Yu,  
59 & Ru, 2010; Karadag, Yang, Ozcelik, & Huang, 2013; Peshkovsky, Peshkovsky, & Bystryak,  
60 2013; Tadros, Izquierdo, Esquena, & Solans, 2004). For all these reasons, nanoemulsions  
61 have an increasing interest in the food, cosmetic and pharmaceutical industries.

62 Different factors, such as the type of oil and surfactant, and process conditions, influence the  
63 physicochemical properties of nanoemulsions (Einhorn-Stoll, Weiss, & Kunzek, 2002;

64 McClements, 2011). The composition of the dispersed oily phase considerably influences the  
65 emulsion quality because of the different densities, viscosities and surface-active ingredients  
66 of the different type of oils (Einhorn-Stoll, Weiss, & Kunzek, 2002). Some of the oily phases  
67 that have been used for obtaining nanoemulsions are limonene oil (Jafari, He, & Bhandari,  
68 2007; Li & Chiang, 2012), sunflower oil (Leong, Wooster, Kentish, & Ashokkumar, 2009),  
69 and medium chain triglycerides (Yang, Marshall-Breton, Leser, Sher, & McClements, 2012;  
70 Yuan, Gao, Mao, & Zhao, 2008). These oily phases are in most cases used to dissolve  
71 bioactive compounds; however, wheat bran oil obtained by SFE already contains highly  
72 bioactive compounds, hence, in this work, WBO will be directly emulsified.

73 The specific objective of the present work was to optimize some process variables, such as oil  
74 concentration, surfactant type and concentration, and emulsification method, to obtain stable  
75 wheat bran oil-in-water (O/W) nanoemulsions with the minimum possible droplet size.  
76 Response surface methodology (RSM) was applied to detect the optimal conditions.  
77 Additionally, emulsion stability along time, antioxidant activity and inhibitory effect of the  
78 optimal nanoemulsion on mushroom tyrosinase, were evaluated.

## 79 **2. Experimental section**

### 80 2.1. Materials

81 *Oil phase:* wheat bran oil was obtained by SFE in a semi-pilot plant at  $25.0 \pm 0.1$  MPa,  
82  $40 \pm 2$  °C and  $8 \pm 1$  kg CO<sub>2</sub>/h. Co-extracted water was separated from WBO by centrifugation  
83 at 12857g during 30 minutes. This WBO was fairly rich in some bioactive compounds such as  
84 alkylresorcinols (47 mg/g), mainly 5-(n-nonadecyl)resorcinol (14.3 mg/g) and 5-(n-  
85 uneicosyl)resorcinol (22.4 mg/g),  $\alpha$ -linolenic acid (37 mg/g), steryl ferulates (18 mg/g),  
86 tocopherols (7 mg/g) and phenolic compounds (25 ppm). A wider characterization of the

87 WBO used in this work, including fatty acid profile, has been reported elsewhere (Rebolleda,  
88 Beltrán, Sanz, González-Sanjosé, & Solaesa, 2013; Rebolleda, Beltrán, Sanz, & González-  
89 SanJosé, 2014) WBO was stored at -20 °C until the emulsification experiments were  
90 performed.

91 *Surfactants:* Several food grade surfactants have been selected in order to achieve the  
92 stabilization of O/W nanoemulsions. Table 1 compiles the different surfactants and mixtures  
93 of surfactants used, together with their HLB (hydrophilic-lipophilic balance) number. Tween  
94 80 (polyoxyethylene (20) sorbitan monooleate) and Span 80 (sorbitan monooleate) were  
95 supplied by Sigma-Aldrich Co. (St. Louis, MO, USA), Tween 20 (polyoxyethylene (20)  
96 sorbitan monolaurate) by Panreac (Barcelona, Spain) and DATEM (diacetyl tartaric acid ester  
97 of mono- and diglycerides) by EPSA (Valencia, Spain).

98 *Water phase:* milli-Q water (Millipore, Billerica, MA, USA) was used for preparing all the  
99 emulsions.

100 *Reactants used for determining antioxidant and tyrosinase inhibition activities:* ABTS (2,2'-  
101 azino-bis (3-ethylbenzothiazoline-6-sulfonic acid) diammonium salt), Trolox (6-hydroxy-  
102 2,5,7,8-tetramethylchromane-2-carboxylic acid), DPPH (2,2-diphenyl-1-picrylhydrazyl) and  
103 TPTZ (2,4,6-Tri(2-pyridyl)-s-triazine), L-DOPA (3,4-dihydroxy-L-phenylalanine) and  
104 mushroom tyrosinase are from Sigma–Aldrich Co. (St. Louis, MO, USA).  $K_2O_8S_2$ ,  $FeCl_3$  and  
105  $FeSO_4$  are from Panreac (Barcelona, Spain).

## 106 2.2. Equipment and procedure

107 A vortex (VWR, Radnor, PA, USA), a high speed blender (Micra D9 equipped with a DS-  
108 5/K-1 rotor-stator, ART Labortechnik, Mülheim, Germany), an ultrasonic bath (Selecta  
109 Ultrasounds H, Barcelona, Spain) and a high intensity ultrasonic processor (Sonics VCX 500,

110 Newtown, CT, USA) were the apparatuses used for preparing the emulsions. The high  
111 intensity ultrasonic processor (500 W, 20 kHz) was used with a titanium alloy microtip probe  
112 of 3 mm diameter, at 20% amplitude and in pulses of 5 seconds (5 s ultrasound and 5 s pause)  
113 to avoid heating of the sample.

114 To prepare an emulsion, WBO and surfactant were mixed before water milli-Q was added.  
115 Quantities of each emulsion ingredient were measured using an analytical balance (Sartorius,  
116 accurate  $\pm 0.0001$ ). The characterization of the emulsions was performed an hour after  
117 emulsification to avoid any creaming or coalescence effect.

### 118 2.3. Nanoemulsions characterization

119 Droplet size distribution, mean droplet diameter and polydispersity index (PDI) of samples  
120 were measured by dynamic light scattering (DLS) using a Zetasizer Nano ZS apparatus  
121 (Malvern Instruments Ltd., UK). The apparatus is equipped with a He-Ne laser emitting at  
122 633 nm and with a 4.0 mW power source. The instrument uses a backscattering configuration  
123 where detection is done at a scattering angle of 173°. Samples were first diluted 1:100 to  
124 avoid multiple scattering effects and then 2 mL samples were poured into DTS0012 square  
125 disposable polystyrene cuvettes. Measurements were performed at 20 °C. The hydrodynamic  
126 diameter was calculated using the Stokes-Einstein equation with the assumption that the  
127 particles were monodisperse spheres.

128 Zeta potential was measured using the aforementioned Zetasizer Nano ZS apparatus. The  
129 measurement was conducted for each diluted sample at 20 °C using DTS1061 disposable  
130 folded capillary cells. The Zeta potential,  $\zeta$ , was calculated from oil droplet electrophoretic  
131 mobility measurements in an applied electric field using the Smoluchowski approximation.

132 The refractive index of the dispersed phase, WBO, was experimentally determined (Milton  
133 Roy abbe-type refractometer, Ivyland, PA, USA) resulting to be 1.476 at 25 °C.

134 The pH of the nanoemulsions was measured by means of a glass pH electrode (Crison,  
135 Barcelona, Spain).

136 Turbidity analysis of the formulated emulsions was carried out by measuring the absorbance  
137 of undiluted samples at 600 nm (Hitachi U-2000 spectrophotometer, Tokyo, Japan) (Ghosh,  
138 Mukherjee, & Chandrasekaran, 2013).

#### 139 2.4. Evaluation of nanoemulsions stability

140 Stability of wheat bran oil in water nanoemulsions was measured in terms of their droplet  
141 growth ratio. Since emulsions tend to aggregate during storage, the droplet size of the  
142 emulsions obtained in this work was measured at 15 and 30 days at the bottom of the cell  
143 containing them. Two different storage conditions were evaluated: 4 °C and darkness and  
144 20 °C and lightness.

145 Additionally, optical characterization of creaming stability was made for the optimal  
146 nanoemulsion using a Turbiscan Lab Expert equipment (Formulaction Co., L'Union, France)  
147 by static multiple light scattering (MLS), sending a light beam from an electroluminescent  
148 diode ( $\lambda = 880$  nm) through a cylindrical glass cell containing the sample. The nanoemulsion  
149 sample without dilution was placed in a cylindrical glass cell and two synchronous optical  
150 sensors received the light transmitted through the sample (180° from the incident light) and  
151 the light backscattered by the droplets in the sample (45° from the incident light). The optical  
152 reading head scans the height of the sample in the cell (about 40 mm), by acquiring  
153 transmission and backscattering data every 40  $\mu$ m. Transmitted and backscattered light were

154 monitored as a function of time and cell height for 60 days at 25 °C (Allende, Cambiella,  
155 Benito, Pazos, & Coca, 2008).

## 156 2.5. Evaluation of nanoemulsions antioxidant activity

157 Antioxidant properties of optimal WBO nanoemulsions were evaluated by using the ABTS,  
158 DPPH and FRAP methods (Rebolleda, Beltrán, Sanz, González-Sanjosé, & Solaesa, 2013;  
159 Rebolleda, Beltrán, Sanz, & González-SanJosé, 2014).

160 *ABTS*: The radical was produced by reaction of 7 mM solution of ABTS in water with  
161 2.45 mM  $K_2O_8S_2$  (1:1) during 16 h at room temperature and darkness (Rivero-Pérez, Muñiz,  
162 & González-Sanjosé, 2007). 20  $\mu$ L of nanoemulsion were mixed with 980  $\mu$ L of radical  
163  $ABTS^{*+}$  previously diluted until obtaining 0.8 absorbance units at 734 nm (Hitachi U-2000  
164 spectrophotometer). The discoloration produced after 20 min reaction is directly correlated  
165 with the antioxidant capacity of the products. Trolox was used as standard compound.

166 *DPPH*: 20  $\mu$ L of nanoemulsion were mixed with 980  $\mu$ L of  $DPPH^*$  solution (50.7  $\mu$ M). The  
167 absorbance at 517 nm was measured after 60 min reaction at ambient temperature and  
168 darkness. The discoloration produced is directly correlated with the antioxidant capacity of  
169 the products. Trolox was used as standard compound.

170 *FRAP*: The FRAP reagent was prepared by mixing 25 mL of 0.3 M sodium acetate buffer  
171 solution at pH 3.6, 2.5 mL of a 10 mM solution of TPTZ dissolved in HCl 40 mM, 2.5 mL of  
172  $FeCl_3$  (20 mM), and 3 mL of milli-Q water. 30  $\mu$ L of nanoemulsions were mixed with 970  $\mu$ L  
173 of FRAP reagent. The reaction was carried out at 37 °C during 30 minutes and the absorbance  
174 was measured at 593 nm (Hitachi U-2000 spectrophotometer).  $FeSO_4$  was used for  
175 calibration. The reductive power of the nanoemulsions was expressed as  $\mu$ mol Fe (II).



176 2.6. Determination of tyrosinase inhibition activity

177 The effect of the nanoemulsions on the *o*-diphenolase activity was monitored by the formation  
178 of dopachrome at 490 nm. The reaction medium (0.2 mL) contained 0.5 mM L-DOPA  
179 prepared in a 100 mM phosphate buffer of pH 7; 0.1 mg/mL of mushroom tyrosinase also  
180 prepared in a 100 mM phosphate buffer of pH 7; and different concentrations (0.5 to 2.5 %,   
181 v/v) of the nanoemulsion. The absorbance at 490 nm was continuously monitored over a time  
182 period of 5 minutes (Labsystems Multiskan MS microplate reader). The initial reaction rate in  
183 the presence or absence of the nanoemulsions was calculated from the slope of the reaction  
184 curve and the inhibition (%) of the nanoemulsions was calculated as follows:

$$185 \quad \% \text{ Inhibition} = [1 - (V_i - V / V_o - V)] \times 100 \quad (1)$$

186 where  $V_i$  and  $V_o$  are the initial reaction rates in the presence or absence of nanoemulsion  
187 respectively and  $V$  is the initial reaction rate in the absence of mushroom tyrosinase.

188 The concentration of nanoemulsion that causes 50% enzyme inhibition ( $IC_{50}$ ) was estimated  
189 by plotting the experimental data of inhibition (%) vs. nanoemulsion concentration.

190 2.7. Experimental design

191 The effect of two of the factors under study, surfactant type and emulsification procedure, on  
192 emulsion formation was firstly studied. Then, response surface methodology (RSM) and  
193 central composite design (CCD) were used to study the effect of oil and emulsifier  
194 concentration and emulsification time, on the droplet size of the nanoemulsions.

195 The experiments performed to select the surfactant are presented in Table 1. Emulsions of  
196 wheat bran oil (1% w/w) with different emulsifiers (1% w/w) were obtained working with the  
197 high speed blender at 29000 rpm during 5 minutes. Each experiment was replicated twice.

198 The emulsification method was selected by preparing different emulsions of wheat bran oil  
199 (1% w/w) using the surfactant (1% w/w) selected in the previous assays. The emulsification  
200 procedures used in each experiment are shown in Table 2. Each experiment was replicated  
201 twice.

202 After selecting the surfactant type and emulsification method, response surface methodology  
203 (RSM) was used to study the effect of oil concentration ( $X_1$ : 1-10% w/w), emulsifier  
204 concentration ( $X_2$ : 1-10% w/w) and ultrasonication time ( $X_3$ : 50-300 s) on the droplet size of  
205 the nanoemulsions ( $Y$ ). A central composite design (CCD) with three levels of each  
206 independent variable (Table 3) was used. The model generated 17 experimental settings with  
207 three replicates in the central point. The design was carried out by duplicate.

208 A low degree polynomial equation (second-order one) was used to express predicted  
209 responses ( $Y$ ) as a function of the independent variables under study ( $X_1$ ,  $X_2$  and  $X_3$ ). The  
210 model equation is as follows:

$$\begin{aligned} 211 \quad Y = & a_0 + a_1 X_1 + a_2 X_2 + a_3 X_3 + a_{11} X_1^2 + a_{22} X_2^2 + a_{33} X_3^2 + a_{12} X_1 X_2 + \\ 212 \quad & a_{13} X_1 X_3 + a_{23} X_2 X_3 \end{aligned} \quad (2)$$

213 where  $Y$  represents the response variable (droplet size in this case),  $a_0$  is a constant, and  $a_i$ ,  $a_{ii}$ ,  
214  $a_{ij}$  are the linear, quadratic and interactive coefficients, respectively. The significance of each  
215 estimated regression coefficient was assessed through values of the statistic parameters,  $F$  and  
216  $p$  (*probability*). The experimental design and data analysis were performed using  
217 STATGRAPHICS Centurion XVI (Statpoint Technologies, Inc., Warrenton, VA, USA).

## 218 2.8. Statistical analysis

219 Experimental data were analyzed by simple statistic parameters in order to detect anomalous  
220 data and to express results through the average values and the corresponding standard  
221 deviation.

222 Analysis of variance (ANOVA) and LSD test were applied to detect the effect factor and the  
223 statistically significant differences among values, respectively.

224 Data analysis was performed using STATGRAPHICS Centurion XVI (Statpoint  
225 Technologies, Inc., Warrenton, VA, USA).

## 226 **3. Results and discussion**

### 227 3.1. Influence of surfactant type on nanoemulsion droplet size.

228 The type of surfactant or mixture of surfactants used for formulating the different emulsions  
229 prepared for this study is presented in Table 1 together with their HLB number. Table 1 also  
230 shows the droplet size and PDI of the emulsions formulated with the different surfactant  
231 systems.

232 ANOVA analysis showed surfactant factor effect and all the analytical values were  
233 statistically different among them. The minimum droplet size ( $84.6 \pm 1.3$  nm) and the  
234 narrowest particle size distribution ( $PDI = 0.257 \pm 0.009$ ) were obtained when the mixture of  
235 Span 80 (37.4%) and Tween 80 (62.6%), with a HLB value of 11, was used. This agrees with  
236 empirical observations that suggest that minimum droplet size and maximum emulsion  
237 stability is obtained for O/W emulsions when using surfactants with a HLB number within the  
238 range 10-12 (McClements, 2005).

239 According to the results obtained in this section, the experiments presented in the next  
240 sections were carried out using the above mentioned surfactant mixture.

### 241 3.2. Influence of the emulsification method on nanoemulsion droplet size

242 The energy needed for the emulsification process can be provided by mechanical agitation,  
243 (e.g.: stirring, high shear mixing), high-pressure homogenization or high power ultrasound  
244 (Huang, Yu, & Ru, 2010; Peshkovsky, Peshkovsky, & Bystryak, 2013). Although high-  
245 pressure homogenization is widely used, ultrasonic methods have several advantages, such as  
246 lower-cost equipment, smaller footprint and easier cleaning and servicing (Peshkovsky,  
247 Peshkovsky, & Bystryak, 2013).

248 Some assays were carried out in order to choose the emulsification method that provided an  
249 emulsion with a small droplet size (Table 2). ANOVA analysis showed emulsification  
250 procedure factor effect. Although the methods using high speed blender happened to bring the  
251 smallest droplet size, samples exhibited visual creaming instability after a few hours of  
252 storage. In contrast, nanoemulsions obtained with the high intensity ultrasonic processor  
253 showed a slightly larger droplet size but visual instability was not observed after the same  
254 storage period. Similar results were obtained by Einhorn-Stoll, Weiss, and Kunzek (2002),  
255 who observed a rapid destabilization of emulsions prepared by a single step with Ultra-turrax.  
256 The ultrasonic bath was considered not suitable for the formation of these nanoemulsions  
257 because, after 10 min, it did not produce the emulsification of the entire oil phase.

258 According to these results, emulsification by high intensity ultrasonication was selected as the  
259 emulsification procedure for the next experiments. However, ultrasonication requires a large  
260 amount of energy when used directly to emulsify two separate phases; therefore, a pre-  
261 emulsification stage might be preferred to first prepare a coarse emulsion (Canselier, Delmas,

262 Wilhelm, & Abismaïl, 2002). In this context, the possibility of adding such a pre-  
263 emulsification step using a vortex or a high speed blender was evaluated. Table 2 shows that  
264 the smallest droplet size ( $111.0 \pm 0.8$  nm) was obtained when this pre-emulsification was  
265 performed using the high speed blender. According to all the results obtained in this section,  
266 emulsification by high intensity ultrasonication preceded by a pre-emulsification with a high  
267 speed blender (29000 rpm, 5 min) was the method selected for carrying out the experiments  
268 presented in the next sections.

269 3.3. Influence of oil and surfactant concentration and ultrasonication time on  
270 nanoemulsions droplet size. Search of the optimal conditions by RSM.

271 The results on the RSM used to optimize the formulation of wheat bran nanoemulsions with  
272 the minimum droplet size, taking into account the process variables, oil and surfactant  
273 concentration and ultrasonication time, are firstly presented. Additionally, stability of the  
274 different nanoemulsions is discussed.

#### 275 3.3.1. *Model fitting*

276 The droplet size of the wheat bran nanoemulsions obtained in the experiments corresponding  
277 to the CCD design is given in Table 3. The experimental data were fitted to a quadratic  
278 polynomial equation, which was able to correctly predict the droplet size of the emulsions.  
279 The model obtained was robust, showed no lack of fit ( $p$  value was higher than 0.05, Table 4)  
280 and a high value of the correlation coefficient ( $R^2 = 0.986$ ) and the distribution of the  
281 residuals was normal. All the coefficients of the quadratic polynomial model (eq. (2)) were  
282 statistically significant ( $p < 0.05$ ) except for the interactive coefficient  $\alpha_{13}$  (Table 4). F values  
283 indicate that, for the range of surfactant concentration studied, the oil content and  
284 ultrasonication time had stronger incidence on the droplet size of the emulsions than the

285 surfactant content. F values also indicate that the interaction with the highest incidence was  
286 the one occurring between the quantity of surfactant and the ultrasonication time.

### 287 3.3.2. *Response surface analysis*

288 In order to study the effect of the independent variables on the droplet size, surface response  
289 and contour plots of the quadratic polynomial model were generated by varying two of the  
290 independent variables within the experimental range while holding the third one constant at  
291 the central point. Fig. 1a was generated by varying the oil and surfactant content in the  
292 emulsion while holding constant the ultrasonication time at 175 s. It shows that, at constant  
293 oil content, an increase of surfactant content between 1 and 7% (w/w) results in a decrease of  
294 droplet size of the emulsion, while a surfactant content higher than 7% results in a droplet size  
295 increase. This could be explained by the role of the surfactant in the emulsion, since its  
296 concentration determines the total droplet surface area, the diffusion rate and the adsorption  
297 phenomena of the surfactant onto the newly formed droplets. Excessive surfactant content  
298 might lead to a lower diffusion rate of surfactants which can result in the coalescence of the  
299 emulsion droplets (Li & Chiang, 2012).

300 The effect of oil content and ultrasonication time on the droplet size at a fixed surfactant  
301 content of 5.5% can be observed in Fig. 1b. This Figure shows that the droplet size of the  
302 nanoemulsion increases both with ultrasonication time and oil content. Ultrasonication time is  
303 an important emulsification parameter, since it affects the adsorption rate of the surfactants to  
304 the droplet surface and the droplet size distribution (Li & Chiang, 2012). The increase of the  
305 droplet size of the emulsion when the ultrasonication time is increased has been described in  
306 the literature and it is due to the over-processing of the emulsion (Fathi, Mozafari, &  
307 Mohebbi, 2012; Kentish, Wooster, Ashokkumar, Balachandran, Mawson, & Simons, 2008; Li  
308 & Chiang, 2012). This effect makes necessary the optimization of the ultrasonic energy

309 intensity input for the system under study (Chandrapala, Oliver, Kentish, & Ashokkumar,  
310 2012). The same effect of ultrasonication time and surfactant content on the droplet size of the  
311 emulsions, previously discussed, was also observed when holding constant the oil content  
312 (Fig. 1c).

### 313 3.3.3. *Stability of wheat bran oil nanoemulsions*

314 Once the influence of the process variables on the droplet size has been evaluated, it is  
315 important to check if there are some important effects of these variables on emulsion stability,  
316 since this is one of the most important parameters for their application.

317 Zeta potential provides information on emulsion stability and is determined by measuring the  
318 velocity of charged droplets or colloids in an electrical potential field of known strength. Oil  
319 droplets in an O/W emulsion exhibit a net charge at the droplet surface. It is usually a  
320 negative charge, and as described by the Helmholtz theory of the electrical double layer, the  
321 negative charges are aligned or closely bound to the interface. These charges attract  
322 counterions from the bulk solution which give rise to a zone of opposite sign, forming an  
323 electrical double layer that causes oil droplets to repel one another. Hence, zeta potential is an  
324 indication of the repulsive forces between emulsion oil droplets, thus characterizes  
325 coalescence/flocculation capacity of emulsions and reflects its stability (Kumar, Mishra,  
326 Malik, & Satya, 2013). Large zeta potential values (positive or negative) indicate difficulty  
327 for coalescence of droplets and therefore high emulsion stability. The zeta potential of the  
328 emulsions corresponding to the CCD experiments varies from -30 to -40 mV, indicating good  
329 stability.

330 The stability of the emulsions was also evaluated in terms of their droplet size growth and  
331 appearance when they were stored during 15 and 30 days at lightness and ambient

332 temperature and when they were stored at 4 °C and darkness. There was little change in the  
333 droplet size of the emulsions during storage (data not shown) but significant changes in their  
334 appearance were detected in terms of sedimentation. Sedimentation is a reversible  
335 destabilization phenomena in emulsions while modification on the droplet size is an  
336 irreversible one (Abismaïl, Canselier, Wilhelm, Delmas, & Gourdon, 1999). Visual evaluation  
337 of the emulsions formulated in this work showed that sedimentation was higher in the  
338 emulsions with higher oil content. Emulsions stored at 4 °C and darkness showed less  
339 sedimentation than those emulsions stored at ambient temperature and lightness when their  
340 visual appearance was evaluated.

#### 341 3.3.4. *Optimal conditions for preparing wheat bran oil nanoemulsions*

342 The optimal conditions for the emulsification of the WBO used in this work would be those  
343 leading to a stable emulsion with the minimum droplet size. According to the RSM results,  
344 the minimum droplet size (39.4 nm) was predicted to be achieved by combining 1.0% (w/w)  
345 WBO, 7.3% (w/w) surfactant and an ultrasonication time of 50 seconds.

346 It should be noted that the surfactant to oil ratio of the optimal wheat bran emulsion is  
347 relatively high what in practice is not desirable due to economic, sensorial and regulatory  
348 reasons (Qian & McClements, 2011). In any case, this is a minor problem when  
349 nanoemulsions are going to be applied as diluted forms, as in the case of this work, which  
350 objective is obtaining an emulsion with the minimum droplet size in order to improve the  
351 bioavailability of the WBO antioxidant compounds.

352 A confirmation of the results using the optimum conditions (1% oil, 7.3% surfactant and 50 s  
353 ultrasonication) was carried out by performing five replicates. The average droplet size  
354 obtained was of  $39.9 \pm 0.4$  nm. The results showed that there was no significant difference ( $p$



355 > 0.05) between experimental and predicted values. The low PDI obtained ( $0.249 \pm 0.012$ )  
356 indicates a narrow distribution of the droplet size.

### 357 3.4. Characterization of the optimal nanoemulsion

358 Besides determining the average droplet size and PDI of the optimal nanoemulsion some  
359 other parameters were evaluated for further characterization. The zeta potential was found to  
360 be  $-22 \pm 2$  mV and pH  $4.9 \pm 0.1$ . The low turbidity of the optimal nanoemulsion (600 nm  
361 absorbance =  $0.36 \pm 0.01$ ) is related to their small droplet size which is below the detection  
362 limit of the human eye (around 50 nm) (Leong, Wooster, Kentish, & Ashokkumar, 2009).  
363 This fact makes this nanoemulsion suitable for its incorporation into different systems without  
364 altering their visual quality. Also, the stability during storage and the antioxidant and  
365 inhibitory tyrosinase activities of WBO optimal nanoemulsion were evaluated.

#### 366 3.4.1. *Stability along storage*

367 There was no significant change in droplet size for the optimal nanoemulsions after 15 and 60  
368 days of storage at 4°C (Fig. 2a), with no noticeable changes on visual emulsion stability.  
369 However, creaming stability measurements for 60 days at 25°C using the Turbiscan Lab  
370 Expert apparatus (Fig. 2b) showed that there was a slight backscattering increase along time  
371 for the middle zone of the measurement cell, which indicates an increase in droplet size  
372 caused by the coalescence of oil droplets. The formation of a sedimentation front at the  
373 bottom of the sample (about 3 mm of cell height) was also observed during the last days,  
374 indicating a tiny emulsion destabilization at the end of the storage period.

375 3.4.2. *Evaluation of the antioxidant activity*

376 The antioxidant activity of the optimal nanoemulsion was evaluated by the ABTS, DPPH and  
377 FRAP methodologies. The values obtained were found to be  $2729 \pm 89 \mu\text{mol Trolox/L}$   
378 emulsion,  $222 \pm 7 \mu\text{mol Trolox/L}$  emulsion and  $471 \pm 9 \mu\text{mol Fe (II)/L}$  emulsion respectively.

379 In order to compare the antioxidant activity of the O/W nanoemulsions with the antioxidant  
380 activity of the oil without emulsification (Rebolleda, Beltrán, Sanz, & González-Sanjosé,  
381 2013), antioxidant activity of the nanoemulsions has been calculated by mass unit of oil in the  
382 emulsion. The FRAP values obtained for the emulsion were much lower than those obtained  
383 for the non-emulsified oil (around  $49 \mu\text{mol Fe (II)/g}$  oil contained in the nanoemulsions,  
384 against  $228 \mu\text{mol Trolox/g}$  oil without emulsification). However, similar results were  
385 obtained for ABTS values (around  $278 \mu\text{mol Trolox/g}$  oil contained in the nanoemulsions and  
386  $270 \mu\text{mol Trolox/g}$  oil without emulsification) and DPPH values (around  $23 \mu\text{mol Trolox/g}$   
387 oil contained in the nanoemulsions and  $26 \mu\text{mol Trolox/g}$  oil without emulsification). These  
388 results might be explained considering different factors, but the accessibility and affinity of  
389 the analytical reactant for the antioxidant compounds are probably the most important ones. It  
390 is also important to have in mind that the antioxidant capacity of the nanoemulsions is  
391 measured directly while the non-emulsified oil is previously dissolved in ethanol. These  
392 considerations help to understand why DPPH, which is dissolved in methanol, a solvent  
393 capable of dissolving both the non-emulsified oil and the emulsion to form a homogeneous  
394 phase, provides similar values for the emulsion and the non-emulsified oil. On the contrary,  
395 FRAP values are fairly different because both, accessibility and affinity of the analytical  
396 reactant and antioxidant compounds are fairly limited. FRAP reacts only with hydrophilic  
397 compounds, as phenols, and these compounds remain at least partially retained in the  
398 emulsion while they are totally accessible in the non-emulsified oil after being dissolved in

399 ethanol. Finally, the affinity of ABTS with both, lipophilic and hydrophilic types of  
400 antioxidants, (Rivero-Pérez, Muñoz, & González-Sanjosé, 2007) explains the similar values  
401 obtained for the emulsion and the non-emulsified oil in this case.

#### 402 3.4.3. *Determination of tyrosinase inhibition activity*

403 Inhibition of food browning is one of the most constant worries of the food industry. The use  
404 of natural inhibitors of polyphenol oxidases is stimulated by the need to replace the sulfite  
405 agents, commonly applied as food anti-browning agents, since they are related to allergic  
406 reactions. Also, cosmetic and pharmaceutical industries demand tyrosinase inhibitors to  
407 prevent melanin-related health problems in humans (Maisuthisakul & Gordon, 2009).

408 The inhibitory effect of the optimal nanoemulsion on the tyrosinase activity was calculated  
409 according to Equation 1. Under the assay conditions used in this work, the inhibition of the  
410 mushroom tyrosinase depends on the nanoemulsion concentration, ranging from 31 to 54 %  
411 for 0.5 to 2.5 % of nanoemulsion concentration. The  $IC_{50}$  for the optimal nanoemulsion was  
412 estimated from the inhibition experimental data and was found to be 2.3% (v/v). This value  
413 corresponds to an oil content of 222.1  $\mu\text{g}$  oil/mL and to an alkylresorcinol content of 10.39  $\mu\text{g}$   
414 AR/mL. Zhuang, Hu, Yang, Liu, Qiu, Zhou, et al. (2010) studied the inhibitory kinetics of  
415 cardol triene (C15:3), a resorcinolic lipid isolated from cashew nut shell, on mushroom  
416 tyrosinase. These authors found that cardol triene was a powerful inhibitor showing an  $IC_{50}$   
417 value of 7.1  $\mu\text{g}/\text{mL}$ . It must be pointed out that no comparison for  $IC_{50}$  values can be easily  
418 established since different experimental conditions have been used. Additionally, each  
419 antioxidant exhibits different inhibition capacity and it is also well-known that isolated  
420 substances and substances included in complex matrices, as is the case of WBO, usually do  
421 not show the same antioxidant capacity. Therefore, further studies are necessary to establish  
422 the mechanism and the inhibition kinetics of wheat bran oil nanoemulsions.

#### 423 **4. Conclusions**

424 Wheat bran oil can be successfully incorporated into water systems by the formulation of  
425 nanoemulsions. Optimization of process conditions by RSM showed that nanoemulsions with  
426 a droplet size of 40 nm can be obtained with a combination of high speed blender (29000  
427 rpm- 5 min) and ultrasonic processor (50 seconds) using 1% of WBO and 7.3% of a  
428 surfactant mixture (Span 80 (37.4%) and Tween 80 (62.6%)). Nanoemulsions showed good  
429 stability when stored at 4°C during 60 days and only a small destabilization was observed in  
430 the last days of the storage when stored at 25°C during 60 days.

431 Nanoemulsions prepared under the reported conditions showed relevant antioxidant properties  
432 when they were evaluated by different methods. Furthermore, results showed that  
433 nanoemulsions could have an inhibitory effect on mushroom tyrosinase activity.

#### 434 **5. Acknowledgments**

435 This work is part of the GALANG project (Ref.: ITC-20113029) financed by the Spanish  
436 Government through CDTI. The authors gratefully acknowledge to the Department of  
437 Chemical and Environmental Engineering of the University of Oviedo (Spain) the opportunity  
438 of using the Turbiscan Lab Expert equipment. S.R. acknowledges the PIRTU program of the  
439 JCyL Education Ministry and the European Social Fund.

#### 440 **References**

441 Abismaïl, B., Canselier, J. P., Wilhelm, A. M., Delmas, H., & Gourdon, C. (1999).  
442 Emulsification by ultrasound: drop size distribution and stability. *Ultrasonics*  
443 *Sonochemistry*, 6(1–2), 75-83.

- 444 Allende, D., Cambiella, Á., Benito, J. M., Pazos, C., & Coca, J. (2008). Destabilization-  
445 enhanced centrifugation of metalworking oil-in-water emulsions: effect of  
446 demulsifying agents. *Chemical Engineering & Technology*, 31(7), 1007-1014.
- 447 Canselier, J. P., Delmas, H., Wilhelm, A. M., & Abismaïl, B. (2002). Ultrasound  
448 emulsification—an overview. *Journal of Dispersion Science and Technology*, 23(1-3),  
449 333-349.
- 450 Chandrapala, J., Oliver, C., Kentish, S., & Ashokkumar, M. (2012). Ultrasonics in food  
451 processing. *Ultrasonics Sonochemistry*, 19(5), 975-983.
- 452 Chen, Q.-X., Song, K.-K., Qiu, L., Liu, X.-D., Huang, H., & Guo, H.-Y. (2005). Inhibitory  
453 effects on mushroom tyrosinase by *p*-alkoxybenzoic acids. *Food Chemistry*, 91(2),  
454 269-274.
- 455 Einhorn-Stoll, U., Weiss, M., & Kunzek, H. (2002). Influence of the emulsion components  
456 and preparation method on the laboratory-scale preparation of o/w emulsions  
457 containing different types of dispersed phases and/or emulsifiers. *Food / Nahrung*,  
458 46(4), 294-301.
- 459 Fathi, M., Mozafari, M. R., & Mohebbi, M. (2012). Nanoencapsulation of food ingredients  
460 using lipid based delivery systems. *Trends in Food Science & Technology*, 23(1), 13-  
461 27.
- 462 Ghosh, V., Mukherjee, A., & Chandrasekaran, N. (2013). Ultrasonic emulsification of food-  
463 grade nanoemulsion formulation and evaluation of its bactericidal activity. *Ultrasonics*  
464 *Sonochemistry*, 20(1), 338-344.

- 465 Herrero, M., Cifuentes, A., & Ibañez, E. (2006). Sub- and supercritical fluid extraction of  
466 functional ingredients from different natural sources: Plants, food-by-products, algae  
467 and microalgae: A review. *Food Chemistry*, 98(1), 136-148.
- 468 Huang, Q., Yu, H., & Ru, Q. (2010). Bioavailability and delivery of nutraceuticals using  
469 nanotechnology. *Journal of Food Science*, 75(1), R50-R57.
- 470 Jafari, S. M., He, Y., & Bhandari, B. (2007). Production of sub-micron emulsions by  
471 ultrasound and microfluidization techniques. *Journal of Food Engineering*, 82(4),  
472 478-488.
- 473 Karadag, A., Yang, X., Ozcelik, B., & Huang, Q. (2013). Optimization of preparation  
474 conditions for quercetin nanoemulsions using response surface methodology. *Journal*  
475 *of Agricultural and Food Chemistry*, 61(9), 2130-2139.
- 476 Kentish, S., Wooster, T. J., Ashokkumar, M., Balachandran, S., Mawson, R., & Simons, L.  
477 (2008). The use of ultrasonics for nanoemulsion preparation. *Innovative Food Science*  
478 *& Emerging Technologies*, 9(2), 170-175.
- 479 Kumar, P., Mishra, S., Malik, A., & Satya, S. (2013). Preparation and characterization of  
480 *Mentha x piperita* oil emulsion for housefly (*Musca domestica L.*) control. *Industrial*  
481 *Crops and Products*, 44(0), 611-617.
- 482 Leong, T. S. H., Wooster, T. J., Kentish, S. E., & Ashokkumar, M. (2009). Minimising oil  
483 droplet size using ultrasonic emulsification. *Ultrasonics Sonochemistry*, 16(6), 721-  
484 727.

- 485 Li, P.-H., & Chiang, B.-H. (2012). Process optimization and stability of D-limonene-in-water  
486 nanoemulsions prepared by ultrasonic emulsification using response surface  
487 methodology. *Ultrasonics Sonochemistry*, 19(1), 192-197.
- 488 Maisuthisakul, P., & Gordon, M. H. (2009). Antioxidant and tyrosinase inhibitory activity of  
489 mango seed kernel by product. *Food Chemistry*, 117(2), 332-341.
- 490 McClements, D. J. (2005). *Food emulsions: principles, practice, and techniques* (2nd ed.).  
491 Boca Raton.
- 492 McClements, D. J. (2011). Edible nanoemulsions: fabrication, properties, and functional  
493 performance. *Soft Matter*, 7(6), 2297-2316.
- 494 Peshkovsky, A. S., Peshkovsky, S. L., & Bystryak, S. (2013). Scalable high-power ultrasonic  
495 technology for the production of translucent nanoemulsions. *Chemical Engineering  
496 and Processing: Process Intensification*, 69(0), 77-82.
- 497 Qian, C., & McClements, D. J. (2011). Formation of nanoemulsions stabilized by model food-  
498 grade emulsifiers using high-pressure homogenization: Factors affecting particle size.  
499 *Food Hydrocolloids*, 25(5), 1000-1008.
- 500 Rebolleda, S., Beltrán, S., Sanz, M. T., & González-Sanjosé, M. L. (2013). Supercritical fluid  
501 extraction of wheat bran oil: characterization and evaluation of antioxidant activity. In  
502 *13th International Conference on Antioxidants*. Marrakech (Morocco).
- 503 Rebolleda, S., Beltrán, S., Sanz, M. T., & González-SanJosé, M. L. (2014). Supercritical fluid  
504 extraction of wheat bran oil. Study of extraction yield and oil quality. *European  
505 Journal of Lipid Science and Technology*, 116, 319–327.

- 506 Rebolleda, S., Beltrán, S., Sanz, M. T., González-Sanjosé, M. L., & Solaesa, Á. G. (2013).  
507 Extraction of alkylresorcinols from wheat bran with supercritical CO<sub>2</sub>. *Journal of*  
508 *Food Engineering*, 119(4), 814-821.
- 509 Rivero-Pérez, M. D., Muñiz, P., & González-Sanjosé, M. L. (2007). Antioxidant profile of red  
510 wines evaluated by total antioxidant capacity, scavenger activity, and biomarkers of  
511 oxidative stress methodologies. *Journal of Agricultural and Food Chemistry*, 55,  
512 5476-5483.
- 513 Roldán, E., Sánchez-Moreno, C., de Ancos, B., & Cano, M. P. (2008). Characterisation of  
514 onion (*Allium cepa* L.) by-products as food ingredients with antioxidant and  
515 antibrowning properties. *Food Chemistry*, 108(3), 907-916.
- 516 Tadros, T., Izquierdo, P., Esquena, J., & Solans, C. (2004). Formation and stability of nano-  
517 emulsions. *Advances in Colloid and Interface Science*, 108–109(0), 303-318.
- 518 Wu, L.-c., Chang, L.-H., Chen, S.-H., Fan, N.-c., & Ho, J.-a. A. (2009). Antioxidant activity  
519 and melanogenesis inhibitory effect of the acetonc extract of *Osmanthus fragrans*: A  
520 potential natural and functional food flavor additive. *LWT - Food Science and*  
521 *Technology*, 42(9), 1513-1519.
- 522 Yang, Y., Marshall-Breton, C., Leser, M. E., Sher, A. A., & McClements, D. J. (2012).  
523 Fabrication of ultrafine edible emulsions: Comparison of high-energy and low-energy  
524 homogenization methods. *Food Hydrocolloids*, 29(2), 398-406.
- 525 Yuan, Y., Gao, Y., Mao, L., & Zhao, J. (2008). Optimisation of conditions for the preparation  
526 of  $\beta$ -carotene nanoemulsions using response surface methodology. *Food Chemistry*,  
527 107(3), 1300-1306.



528 Zhuang, J.-X., Hu, Y.-H., Yang, M.-H., Liu, F.-J., Qiu, L., Zhou, X.-W., & Chen, Q.-X.  
529 (2010). Irreversible competitive inhibitory kinetics of cardol triene on mushroom  
530 tyrosinase. *Journal of Agricultural and Food Chemistry*, 58(24), 12993-12998.

531

532

## Figure Captions

Figure 1. Response surface and contour plots of the combined effects of oil and surfactant content and ultrasonication time on the droplet size of the wheat bran nanoemulsions: (a) oil and surfactant content at an ultrasonication time of 175 s; (b) oil content and ultrasonication time at a surfactant content of 5.5%; (c) surfactant content and ultrasonication time at an oil content of 5.5%.

Figure 2. Optimal nanoemulsion prepared with 1% of WBO, 7.2% Span 80:Tween 80 (37.4:62.6) and 50 seconds of ultrasounds: (a) droplet size distribution after 0, 15 and 60 days of storage at 4 °C and darkness, (b) backscattering profiles during 60 days of storage at 25°C and darkness.

Table 1. Surfactants used for the emulsification of WBO, their HLB numbers and mean droplet size and polydispersity index (PDI) of the emulsions obtained

Surfactant	HLB number	Droplet size (nm)	PDI
Tween 20	16.7	200.0 ± 8.1 <sup>d</sup>	0.352 ± 0.016
Tween 80	15.0	109.9 ± 6.6 <sup>b</sup>	0.370 ± 0.009
DATEM	8.0	393.2 ± 8.0 <sup>e</sup>	0.485 ± 0.011
Span 80:Tween 80 (37.4:62.6)	11.0	84.6 ± 1.3 <sup>a</sup>	0.257 ± 0.009
Span 80:Tween 80 (75:25)	7.0	171.1 ± 3.9 <sup>c</sup>	0.280 ± 0.012

Values with different letters in each column are significantly different (LSD test,  $p < 0.05$ )

Table 2. Equipment and conditions used for the emulsification of WBO and mean droplet size and polydispersity index (PDI) of the emulsions obtained

Pre-emulsification step		Emulsification step		Droplet size (nm)	PDI
Method	Time (min)	Method	Time (min)		
None		High speed blender 25000 rpm	5.0	95.6 ± 1.6 <sup>c</sup>	0.234 ± 0.008 <sup>c</sup>
None		High speed blender 29000 rpm	5.0	77.0 ± 1.1 <sup>b</sup>	0.225 ± 0.013 <sup>c</sup>
None		High speed blender 35000 rpm	5.0	66.3 ± 0.9 <sup>a</sup>	0.187 ± 0.005 <sup>b</sup>
None		Ultrasonic bath	10	-	-
None		High intensity ultrasonic processor	2.5	136.4 ± 1.3 <sup>e</sup>	0.121 ± 0.010 <sup>a</sup>
Vortex	1	High intensity ultrasonic processor	2.5	133.5 ± 1.3 <sup>e</sup>	0.139 ± 0.009 <sup>a</sup>
High speed blender 29000 rpm	5	High intensity ultrasonic processor	2.5	111.0 ± 0.8 <sup>d</sup>	0.132 ± 0.008 <sup>a</sup>

Values with different letters in each column are significantly different (LSD test,  $p < 0.05$ )

Table 3. Matrix of the central composite design (CCD) and experimental data obtained for the response variable (Y)

Run	Independent variables			Response variable
	WBO concentration (X <sub>1</sub> , % w/w)	Surfactant concentration (X <sub>2</sub> , % w/w)	Ultrasonication time (X <sub>3</sub> , s)	Droplet size (Y, nm) (mean ± SD)
1	5.5	5.5	175	155.7 ± 9.1
2	1.0	1.0	50	81.5 ± 4.2
3	10.0	1.0	50	199.0 ± 0.7
4	1.0	10.0	50	50.7 ± 2.0
5	10.0	10.0	50	138.1 ± 0.8
6	1.0	1.0	300	116.8 ± 6.2
7	10.0	1.0	300	226.1 ± 1.3
8	1.0	10.0	300	143.6 ± 1.8
9	5.5	5.5	175	154.3 ± 4.2
10	10.0	10.0	300	247.3 ± 20.4
11	1.0	5.5	175	92.1 ± 3.4
12	10.0	5.5	175	210.4 ± 15.4
13	5.5	1.0	175	184.8 ± 2.1
14	5.5	10.0	175	174.8 ± 1.2
15	5.5	5.5	50	105.2 ± 1.3
16	5.5	5.5	300	167.4 ± 0.4
17	5.5	5.5	175	149.5 ± 1.3

Table 4. Analyses of variance of the regression coefficients of the quadratic equation (2) for the droplet size of WBO nanoemulsions

Polynomial coefficient (PC) <sup>a</sup>	PC-value	F-value	p-value
$\alpha_0$	58.9453		
$\alpha_1$	16.1043	2384.05	0.0000
$\alpha_2$	-17.6021	24.05	0.0080
$\alpha_3$	0.552472	884.93	0.0000
$\alpha_{11}$	-0.299374	8.17	0.0460
$\alpha_{22}$	1.10803	111.87	0.0005
$\alpha_{33}$	-0.00134799	98.58	0.0006
$\alpha_{12}$	-0.220679	13.25	0.0220
$\alpha_{13}$	0.00181111	0.69	0.4533
$\alpha_{23}$	0.0310333	202.18	0.0001
Lack of fit		2.55	0.1883

<sup>a</sup>  $\alpha_0$  is a constant,  $\alpha_i$ ,  $\alpha_{ii}$  and  $\alpha_{ij}$  are the linear, quadratic and interactive coefficients of the quadratic polynomial equation, respectively

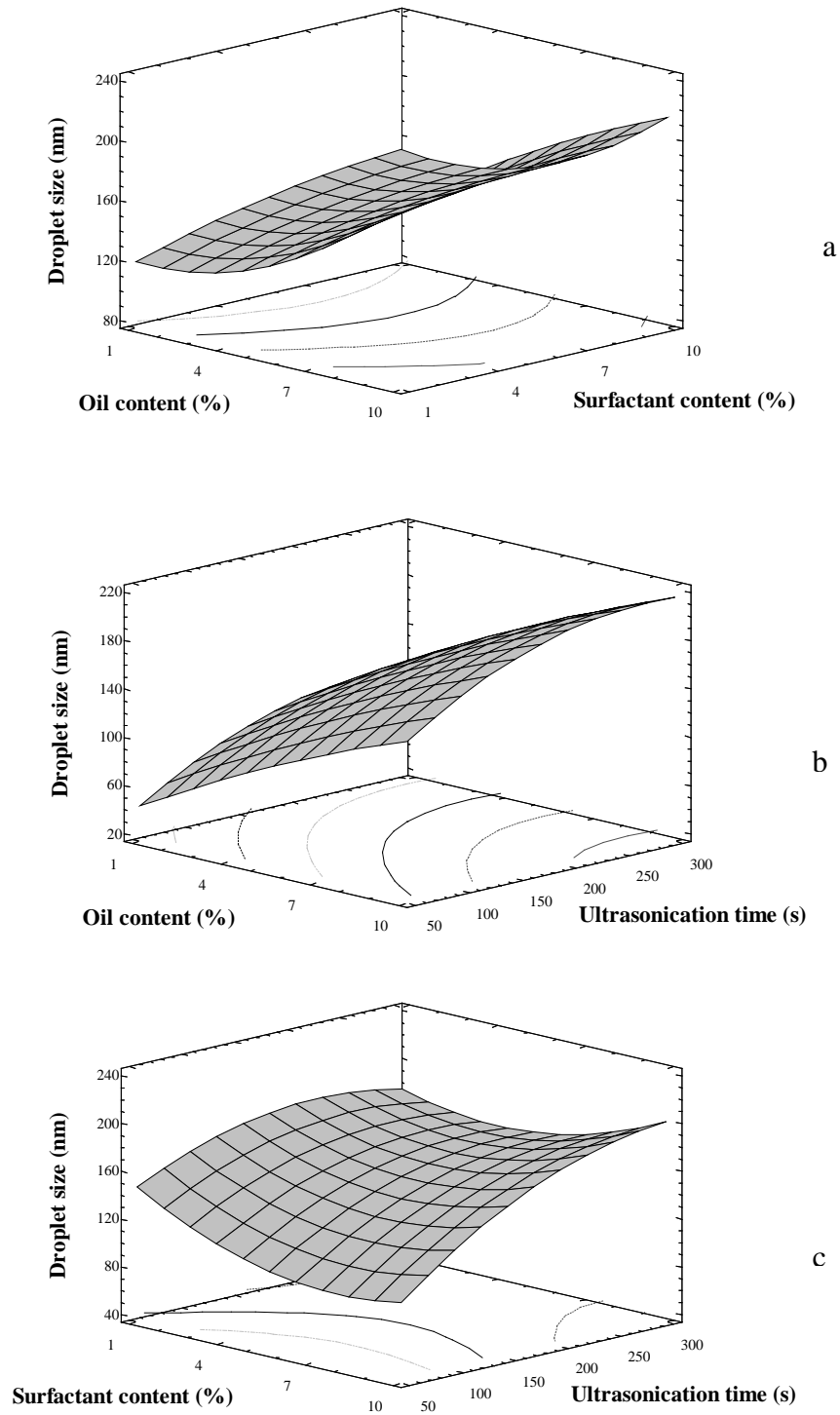
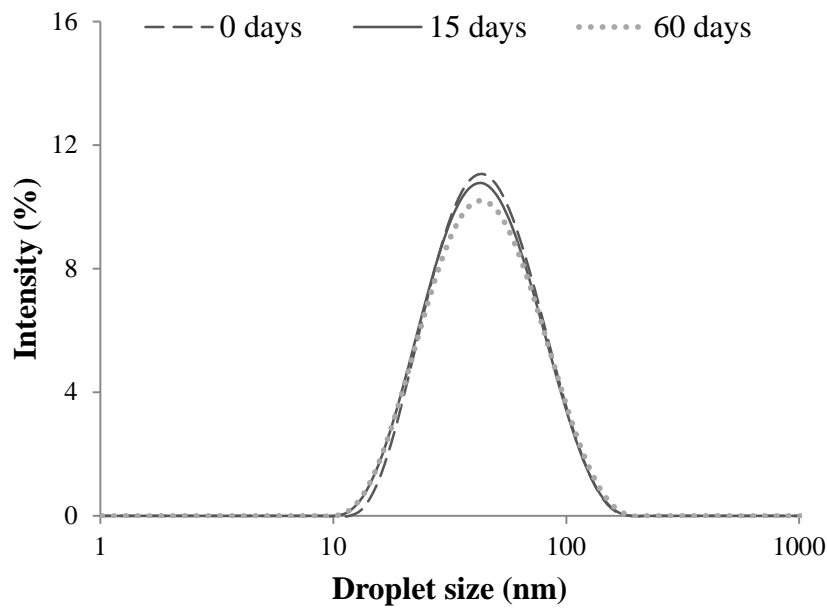
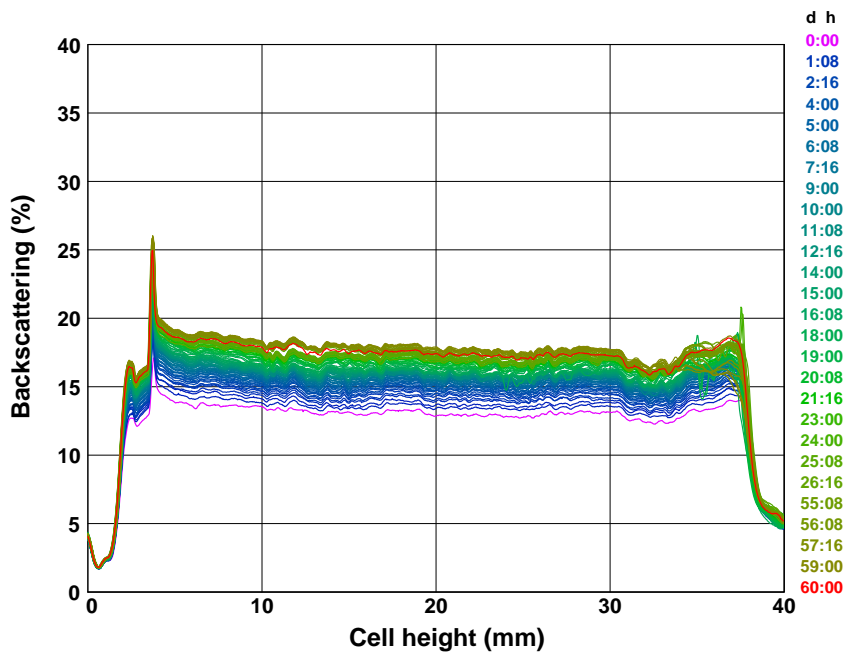


Figure 1. Response surface and contour plots of the combined effects of oil and surfactant content and ultrasonication time on the droplet size of the wheat bran nanoemulsions: (a) oil and surfactant content at an ultrasonication time of 175 s; (b) oil content and ultrasonication time at a surfactant content of 5.5%; (c) surfactant content and ultrasonication time at an oil content of 5.5%.



a



b

Figure 2. Optimal nanoemulsion prepared with 1% of WBO, 7.3% Span 80:Tween 80 (37.4:62.6) and 50 seconds of ultrasounds: (a) droplet size distribution after 0, 15 and 60 days of storage at 4 °C and darkness, (b) backscattering profiles during 60 days of storage at 25°C and darkness.